Available online at www.sciencedirect.com
ScienceDirect
Journal of Hazardous Materials 147 (2007) 449–456
Journal of Hazardous Materials
www.elsevier.com/locate/jhazmat

Activity and leaching features of zinc–aluminum ferrites in catalytic wet oxidation of phenol

Aihua Xu [a,b], Min Yang [a], Ruiping Qiao [a], Hongzhang Du [a], Chenglin Sun [a,*]

[a] *Dalian Institute of Chemical Physics, Chinese Academy of Sciences, Dalian 116023, China*
[b] *Graduate University of the Chinese Academy Sciences, Beijing 100049, China*

Received 23 August 2006; received in revised form 8 November 2006; accepted 8 January 2007
Available online 12 January 2007

Abstract

A series of $ZnFe_{2-x}Al_xO_4$ spinel type catalysts prepared by sol–gel method have been characterized and tested for catalytic wet oxidation (CWO) of phenol with pure oxygen. The iron species existed in these materials as aggregated iron oxide clusters and Fe^{3+} species in octahedral sites. With a decrease in iron content the concentration of the first iron species decreased and the latter increased. Complete phenol conversions and high chemical oxygen demand (COD) removals were obtained for all catalysts during phenol degradation at mild reaction conditions (160 °C and 1.0 MPa of oxygen pressure). Increasing with the concentration of Fe^{3+} species in octahedral sites, induction period became significantly shortened. After phenol was completely degraded, the concomitant recycling of the leaching Fe^{3+} ions back to the catalyst surface was observed, and in this case it is possible to perform successful CWO reactions with some cycles. It is also suggested that during the reaction the Fe^{3+} cations coordinated in octahedral sites in the $ZnFe_{2-x}Al_xO_4$ catalysts are resistant to acid leaching, but the reduced Fe^{2+} cations become much more labile, leading to increased Fe leaching.
© 2007 Elsevier B.V. All rights reserved.

Keywords: Catalytic wet oxidation; Phenol; Leaching; Spinel; Iron; Zinc

1. Introduction

Industry creates large annual amounts of organic wastewater containing products hazardous to the environment, and development of efficient technologies is a need and considerable research efforts are being devoted into this field [1]. The application of advanced oxidation technologies (AOTs) have emerged as an important alternative for the destruction of organic pollutants. These processes basically involve the generation of reactive hydroxyl radials ($OH^{\bullet}$) with high oxide potential, which are able to mineralize these refractory compounds [2,3]. The heterogeneous catalytic AOTs allow a significant reduction of the temperature and pressure employed by the non-catalytic oxidation processes, and avoid the problem of the adsorption regeneration in the adsorption process [3,4]. Iron is a widely available and non-toxic element, and catalytic generation of hydroxyl radials by iron ions is well known [5]. Development of supported iron catalysts is gaining much importance recently in AOTs [6]. In literature studies on immobilized Fe ions different supports have been involved, such as zeolites [7–9], pillared clays [10,11], silica [12], active carbon [1] and ion-exchange resin [13].

The environments of iron species in the iron-containing catalysts are closely related to the strategy of synthesis, and different environments of iron species coexist in the synthesized materials. ESR data indicate that in Al–Fe-pillared clays iron is present as (i) isolated species (in highly distorted octahedral symmetry), probably located on the clay layer; (ii) oxide clusters and (iii) isolated iron species, which probably located on the pillars as extra framework species [10]. The iron species associated to the pillars are much more reactive towards phenol mineralization than the other iron species present in pillared clays [10]. Iron-containing SBA-15 catalyst is a composite material that contains crystalline hematite particles embedded into the mesostructured SBA-15 matrix and well dispersed ionic iron species within the siliceous framework [3].

The solid iron catalysts in AOTs may undergo some deactivation resulted from surface deposition and strong adsorption

* Corresponding author. Tel.: +86 411 84379326; fax: +86 411 84699965.
E-mail address: clsun@dicp.ac.cn (C. Sun).

0304-3894/$ – see front matter © 2007 Elsevier B.V. All rights reserved.
doi:10.1016/j.jhazmat.2007.01.026

of a polymeric carbon layer and from the leaching of the active species of the catalysts [1,8,13,14]. Should the problem of the catalysts lifetime be resolved, the AOTs would find numerous applications. Many works have shown that extraframework aggregated iron oxide clusters, which are retained to the support only by weak Van der Waals bonds, easily leach out into the liquid-phase during reaction; whereas the iron cations incorporated inside the framework, which are attached by covalent bonds, are stable towards leaching [8,15,16]. The stability of catalysts is also strongly dependent on the reaction conditions, including reaction temperature, pH in solution, reaction time, oxidant concentration and composition and concentration of pollutants [1,3,4,8].

Spinels are compounds of the general formula $A^{2+}B_2{}^{3+}O_4$. The structure and properties of spinel have a wide interest in semiconductors, magnetic, refractory materials, pigments and heterogeneous catalysts [17,18]. Recently, Alejandre et al. [19–21] have shown that copper, nickel, and aluminum mixed oxides crystallizing in the spinel form are active and stable catalysts in catalytic wet air oxidation (CWAO) of phenol. In a previous work [22], we studied the influence of partial replacement of Cu by Fe on the CWO of phenol in the $Cu_{0.5-x}Fe_xZn_{0.5}Al_2O_4$ spinel catalysts, and found that the activity and stability of these catalysts increased with Fe content. Zinc ferrite is a normal spinel in which zinc cations are in tetrahedral sites and iron cations are in octahedral sites, and has been widely used in the oxidative dehydrogenation of 1-butene to butadiene [18]. In this paper, the effect of aluminum introduction into $ZnFe_2O_4$ on CWO performance of phenol was investigated in order to develop an effective catalyst with high catalytic activity. As the leaching of active sites is a common problem in liquid-phase oxidation reactions, and the understanding of the nature of such leaching is vital for designing stable catalysts for liquid-phase oxidation, the leaching features of iron species in the $ZnFe_{2-x}Al_xO_4$ spinel type catalysts were also studied.

2. Experimental

2.1. Catalyst preparation and characterization

The $ZnFe_{2-x}Al_xO_4$ spinel type catalysts ($x = 0$, 0.5, 1.0, 1.5, 1.75) were prepared by sol–gel method by mixing stoichiometric amounts of $Zn(NO_3)_2{\cdot}6H_2O$, $Fe(NO_3)_3{\cdot}9H_2O$, $Al(NO_3)_3{\cdot}9H_2O$ and excess citric acid in distilled water. The solutions were heated up to 70 °C in order to remove water, then the resulted gels were kept at 110 °C for 15 h, the final catalysts were obtained by decomposition of the xerogels in an oven at 750 °C for 4 h, and the catalyst particle sizes are 51–90 μm in diameter.

Crystalline structure of the catalysts was analyzed with a Rigaku D/max RB diffractometer using Cu radiation. The X-ray was operated at 40 kV and 40 mA. Average crystallite size was obtained by measuring the broadening of the (3 1 1) spinel diffraction peak and applying the Scherrer equation [$D = 0.89\lambda/\beta(\theta)\cos(\theta)$] [23]. Lattice parameters were calculated from the d-value of the (3 1 1) spinel diffraction peak. The BET surface areas were assessed by N_2 adsorption isotherms at 77 K using a NOVA 4000 instrument. The catalyst samples prior to the adsorption measurement were degassed at 300 °C for 6 h under vacuum. Diffuse reflectance UV–vis spectra were obtained under ambient conditions on a Jasco V-550 UV–vis spectrophotometer in the range of 200–800 nm.

2.2. Catalyst tests

Catalyst testing in the CWO of phenol was carried out in a 1L stainless steel autoclave reactor. The reactor was first filled with 500 ml of 2.0 g/l phenol solution, 2.0 g/l of powdered catalyst and oxygen with a pressure of 1.0 MPa at room temperature which was enough for the stoichiometric amount of phenol to be completely oxidized; then was heated to a temperature of 160 °C. When the set temperature was attained after about 30 min, the reaction was started with impeller stirring at a speed of 600 rpm which was enough to that the external mass transfer effects can be neglected. During reactions representative liquid samples were withdrawn from the reactor, filtered and analyzed with respect to COD, phenol concentration, pH and Fe and/or Zn leaching. After each sample was withdrawn, the decreased oxygen pressure was supplied from the gas cylinder to keep the oxygen pressure constant.

The COD value of the solution was measured following standard determination techniques using potassium dichromate as oxidant. The phenol concentration and product distribution were analyzed by a high performance liquid chromatography equipped with a Hypersil ODS2 column (4.6 mm × 250 mm) and an UV detector at 210 nm. A mixture of methanol (20%), deionized water (80%) and phosphoric acid (0.5%) was used as mobile phase at a flow rate of 1 ml/min. The quantity of zinc ions in the solution was analyzed by ICP-AES spectrometer; the quantity of Fe^{2+} was determined by a colorimetric method using 1,10-phenanthroline reagent with very high sensitivity to Fe^{2+} [24]. Additionally, the total leached iron content was measured by the colorimetric method after Fe^{3+} ions were reduced to Fe^{2+} ions by hydroxylamine hydrochloride.

3. Results and discussion

3.1. Characterization of $ZnFe_{2-x}Al_xO_4$ catalysts

The X-ray diffraction patterns of $ZnFe_{2-x}Al_xO_4$ catalysts are presented in Fig. 1. The characteristics peaks of a single phase with the spinel structure was observed in all samples; and no impurities such as ZnO and Fe_2O_3 were found, which are usually observed when the catalysts prepared by coprecipitation or hydrothermal methods [18,25]. The diffraction peaks for all the catalysts are broad in Fig. 1; and their broadening increases with aluminum content. From the width of the diffraction peaks, the average crystallite sizes were measured and are shown in Table 1. As the crystallite size decreases with the isomorphic substitution of iron by aluminum, one can then expect that surface areas of these catalysts increase with the aluminum content [25]. In Table 1, the corresponding surface area increased from 32 to 59 $m^2\,g^{-1}$. From Fig. 1 it can be also observed that the shift of the peaks position towards upper 2θ angles at increasing alu-

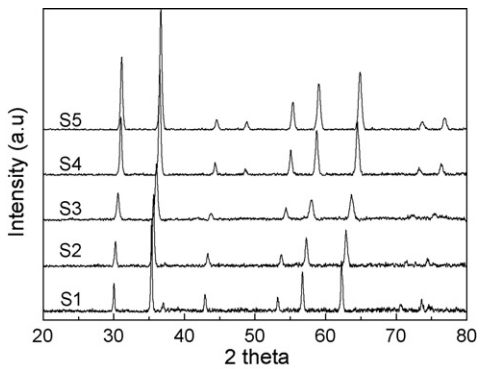

Fig. 1. XRD patterns of $ZnFe_{2-x}Al_xO_4$ catalysts.

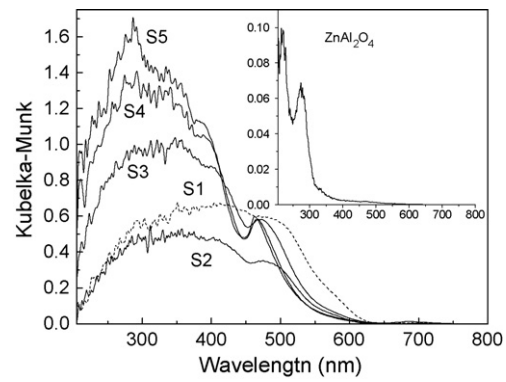

Fig. 3. UV–vis spectra of $ZnFe_{2-x}Al_xO_4$ catalysts.

minum content, indicating that Al atoms have been incorporated into the spinel structure. In order to check whether the solid solution was perfect, the lattice parameters are reported in Table 1, and also plotted against aluminum concentration in Fig. 2, in which the theoretical line of Vegard's law (dot line) is also plotted. It seems that a homogeneous solid solution was obtained in the range of the aluminum concentration $0.5 \leq x \leq 1.75$, since the lattice parameters observed were predicted by Vegard's law [18].

Although the catalysts prepared in this work do not present any segregated phase, they may be present in small amounts under the limitation of XRD detection; if the compounds are microcrystalline or amorphous they are not also observed. Fig. 3 shows the diffuse reflectance UV–vis spectra of the $ZnFe_{2-x}Al_xO_4$ catalysts. The S1 and S2 catalysts exhibited the same behavior as Fe_2O_3, with the observed band appearing between 400 and 600 nm [26], which could be explained by the surface enrichment of iron oxide [27]. Their absorption intensity decreased with decreasing iron content. For the S3, S4 and S5 catalysts, strong and broad adsorption in the region of 280–330 nm with an increase in intensity was observed, indicating an increase of concentration of Fe^{3+} species in octahedral sites [28]. An intensity shoulder centered at 500 nm can be also observed on the three spectra, implying that the extraframework iron was still present [28]. Additionally, as shown in the inset in Fig. 3, $ZnAl_2O_4$ showed two very weak peaks centered at below 300 nm, therefore, Zn^{2+} species has insignificant influence on the analysis of the UV–vis spectra.

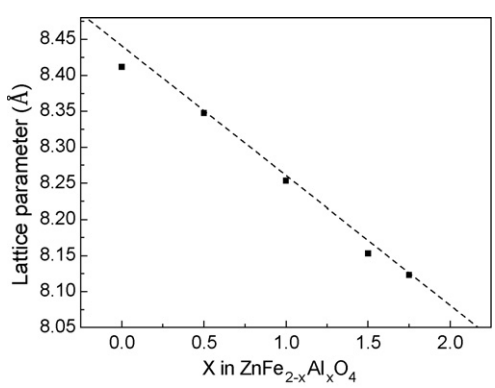

Fig. 2. Lattice parameter of $ZnFe_{2-x}Al_xO_4$ catalysts.

As the resistance to acid attack of the catalysts used in CWO is an important factor for the stability of these solids, and it was reported that iron ions can be fixed by some supports when iron ions incorporated inside the framework [16], the amount of iron leaching from the $ZnFe_{2-x}Al_xO_4$ catalysts dissolution in hydrochloric acid solution was measured, in order to check whether the Fe^{3+} species in octahedral sites was more stable than the extraframework Fe^{3+} species. The experiments were carried out at room temperature with 1.0 g/l of powder catalyst. As shown in Fig. 4, for the S5 catalysts, the amount of iron leaching kept 3.7 ppm during all the reaction time, even in 2 M of hydrochloric acid solution, that only corresponding to a ca. 4.8% loss of the total iron content. However, for the S1 catalyst, the amount of iron leaching increased with reaction time. Moreover, when the concentration of hydrochloric acid solution was changed to 2 M, a remarkable increase of iron leaching was observed. From these results and the above analysis of UV–vis spectra, it can be conjectured that under this acidic condition the extraframework Fe clusters were removed but framework Fe species remained; and we can conclude that when the Fe^{3+} species is incorporated into the spinel structure it becomes more stable.

Table 1
Properties of $ZnFe_{2-x}Al_xO_4$ catalysts

Catalyst	X in $ZnFe_{2-x}Al_xO_4$	Crystallite size (nm)	Lattice parameter (Å)	S_{BET} ($m^2\ g^{-1}$)	Zn leaching (ppm)
S1	0.00	155	8.412	32	16.5
S2	0.50	118	8.348	32	15.9
S3	1.00	81.7	8.254	37	15.2
S4	1.50	61.8	8.153	46	14.3
S5	1.75	55.1	8.123	59	15.7

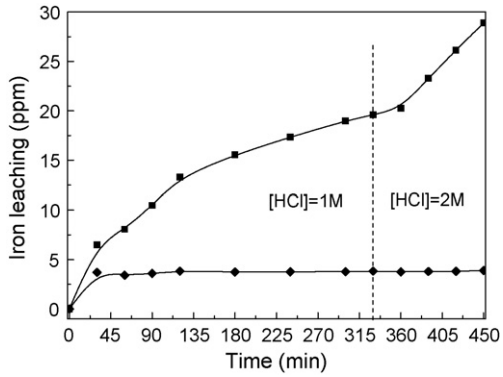

Fig. 4. Evolution of Fe leaching along reaction time with $ZnFe_{2-x}Al_xO_4$ catalysts dissolution in hydrochloric acid (■, S1 and ♦, S5).

3.2. Catalytic activity and stability in degradation of phenol

The efficiency of $ZnFe_{2-x}Al_xO_4$ catalysts in CWO of phenolic aqueous with oxygen was evaluated at 160 °C. Figs. 5 and 6 show the evolution of phenol conversion and COD removal within reaction time, respectively. In the CWO of phenol using solid catalysts, induction period is usually observed and reaction proceeds mostly during 5–60 min after a take-off and steadied out to the final state. As shown in Fig. 5, for the S1 and S2 catalysts, induction period increased from 30 to 120 min; however, for the S3, S4 and S5 catalysts, induction period became significantly shortened from 180, 150 to 5 min. Complete phenol conversions were obtained for the five catalysts after the induction periods; and high COD removals in degrees of more than 90% were observed in Fig. 6. The results of blank test are also shown in Figs. 5 and 6. The date clearly show that in absence of a catalyst the activity was much lower than that of the S1 and S5 catalysts; but higher than that of the S2, S3 and S4 catalysts. Additionally, the catalysts showed poor ability to adsorb phenol as the phenol conversions were nearly to zero when the reactions were started.

The isomorphic substitution of Fe^{3+} by Al^{3+} into the octahedral sites can give rise to a lattice distortion, which facilitates a charge transfer from Fe^{3+} to O^{2-}, increasing the basicity of the oxygen atoms in the Fe–O–Al bonds [18]. Assuming that the Fe^{3+} species in octahedral sites in spinel structure are more active than the aggregated iron oxide clusters on the catalyst surface, the change of induction period for the $ZnFe_{2-x}Al_xO_4$ catalysts can be easily explained. For the S1 and S2 catalysts, induction period increased with decreasing the amount of aggregated iron oxide clusters, which are the main iron species present on the two catalysts surface. For the S3, S4 and S5 catalysts, induction period was mainly influenced by the amount of Fe^{3+} species in octahedral sites, and it decreased with increasing the concentration of Fe^{3+} species in octahedral sites.

Leaching experiments studies of iron and zinc species from the $ZnFe_{2-x}Al_xO_4$ catalysts were also detected. The evolutions of iron concentration dissolved into the aqueous solution within reaction time are illustrated in Fig. 7; and the zinc concentrations after reactions are shown in Fig. 8 and Table 1. From Fig. 7 it can be seen that for all the catalysts the concentrations of iron leaching first increased to the maximum values with reaction time, and then decreased to less than 10 ppm. The maximum values decreased from 38 to 15 ppm with decreases in iron content which were simultaneously detected when phenol was completely degraded. The analogy trends of zinc leaching were not found in Fig. 8 for the S1 and S2 catalysts and they increased within reaction time. In Table 1 the concentrations of zinc leaching were about 15 ppm for all the catalysts.

An extra homogeneous run with both Fe and Zn at concentration of 15 ppm comparable to the maximum leaching conditions of the S5 catalyst was also performed, to indicate how important the homogeneous reaction was. The result is shown in Fig. 9.

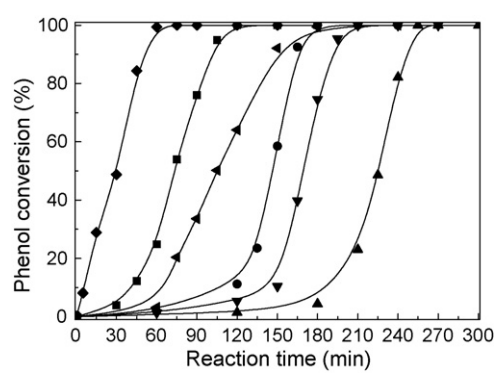

Fig. 5. Evolution of phenol conversion along reaction time in CWO of phenol with $ZnFe_{2-x}Al_xO_4$ catalysts (■, S1; ●, S2; ▲, S3; ▼, S4; ♦, S5; ◄, blank).

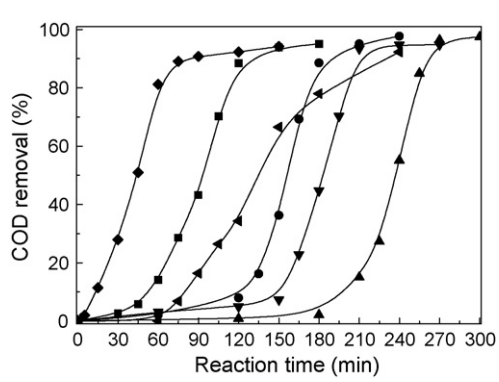

Fig. 6. Evolution of COD removal along reaction time in CWO of phenol with $ZnFe_{2-x}Al_xO_4$ catalysts (■, S1; ●, S2; ▲, S3; ▼, S4; ♦, S5; ◄, blank).

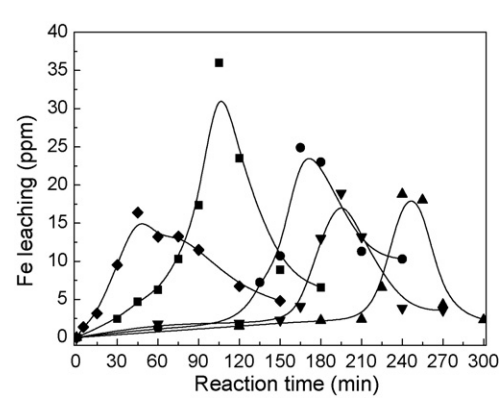

Fig. 7. Evolution of Fe leaching along reaction time in CWO of phenol with $ZnFe_{2-x}Al_xO_4$ catalysts (■, S1; ●, S2; ▲, S3; ▼, S4; ♦, S5).

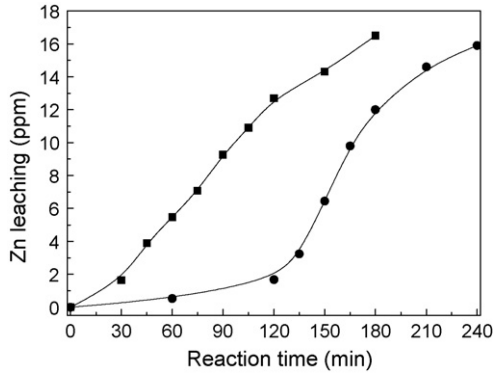

Fig. 8. Evolution of Zn leaching along reaction time in CWO of phenol with S1 and S2 catalysts (■, S1 and ●, S2).

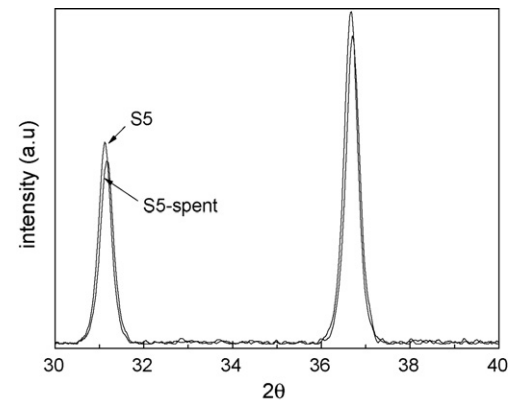

Fig. 10. XRD patterns of fresh and spent $ZnFe_{0.25}Al_{1.75}O_4$ catalysts.

Although the homogenous catalytic reaction was significant, the activity of the solid catalyst cannot be completely attributed to the free metal ions, as the activity of leached metals was lower than that of the S5 catalyst, and the maximum Fe and Zn leaching was not obtained at the beginning of reaction when using the solid catalyst. Moreover, comparing the values of induction time of the five catalysts with the amounts of leached iron and zinc, it can be seen that the catalysts activity is not proportional to the leached iron and zinc ions. Maybe the leaching of iron and zinc in the $ZnFe_{2-x}Al_xO_4$ catalysts is a secondary effect related mainly to the complexing action of reaction intermediates [2].

For the $ZnFe_{0.25}Al_{1.75}O_4$ catalyst showed the highest activity and smallest metal ions leaching in the five catalysts, the catalytic results for the repeated use of the $ZnFe_{0.25}Al_{1.75}O_4$ catalyst were further performed and are shown in Table 2. The procedure of recycling was analyzed as follows: after the CWAO reaction, the catalyst was filtered and then tested again at the same reaction conditions without any further treatment. The cycle was repeated four times. Due to the incomplete recovery of the solid, the amount of catalyst used in these tests was progressively decreasing; notwithstanding this issue, for all the numbers of reaction cycles, an insignificant activity loss was observed; and the catalyst collected after reaction exhibited the original color, indicating that carbonaceous deposits on the catalyst surface was not noticeable. In terms of leaching during the five runs, the amounts of iron and zinc leaching in the final solutions decreased with increasing run times. It is noticed that during the fifth run the evolution of iron leaching showed similar trend to that in the first run and the amount of zinc leaching after the reaction was only 1.53 ppm. The results indicate that the successful CWO reactions with some cycles over the $ZnFe_{0.25}Al_{1.75}O_4$ catalyst could mainly ascribe to iron species, which can return to the catalyst surface after dissolved in solution; zinc species may have insignificant contribution to the oxidation rate, since the obvious decease of zinc leaching had little influence on the rate of oxidation. In fact, if zinc was replaced by other species such as magnesium, the catalyst will show similar activity. XRD patterns were also taken after the first catalytic run. As evidenced in Fig. 10, the structure of the $ZnFe_{0.25}Al_{1.75}O_4$ catalyst was not obviously affected by the reaction, because only little changes in the respective XRD peaks' height were observed.

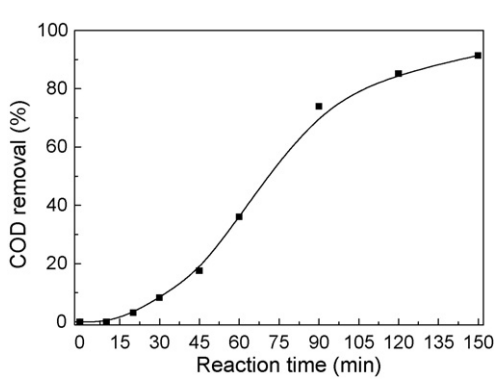

Fig. 9. Evolution of COD removal along reaction time in CWO of phenol with Fe and Zn ions ([Fe] = 15 ppm and [Zn] = 15 ppm).

3.3. Leaching features of $ZnFe_{2-x}Al_xO_4$ catalysts

In all spinels only the octahedrally coordinated cations are exposed to the reactants [29]. The $ZnFe_{2-x}Al_xO_4$ catalysts are normal spinels in which zinc cations are in the tetrahedral sites and iron and aluminum cations are in the octahedral sites [18]. However, zinc leaching during the reactions was observed, probably due to the fact that a small amount of zinc is present on the catalyst surface, which has been detected by LEIS [30]. Many researchers have proposed the reasonable hypothesis of leaching of Fe^{2+} from Fe^{3+} containing catalysts as a result of reduction of Fe^{3+} species [31]. But this hypothesis is not suitable for the zinc leaching, as Zn^{2+} species is more resistant to reduction than Fe^{3+} species in spinel structure [27,32]. It is suggested that zinc leaching can be attributed to acid attack of the surface defects of $ZnFe_{2-x}Al_xO_4$ catalysts, and the rate of acid dissolution is controlled by the number of defects originally present in the oxide surface.

The evolution of iron leaching within reaction time showed different behavior to that of zinc leaching. This is attributed to the special characterization of Fe^{3+} ions, which can be adsorbed in the $ZnFe_{2-x}Al_xO_4$ catalysts surface. Fe^{2+} ions and Zn^{2+} ions cannot be adsorbed by the catalysts, and the amount of zinc leaching increased with reaction time, but Fe^{2+} leaching can decrease through reoxidation to Fe^{3+}. This conclusion is

Table 2
Repeated used of $ZnFe_{0.25}Al_{1.75}O_4$ catalyst in catalytic wet air oxidation of phenol

Number of reaction cycles	Reaction time (min)	X_{phen} (%)	X_{COD} (%)	Fe leaching (ppm)	Zn leaching (ppm)
1	150	100	90.8	4.82	15.7
2	150	100	89.8	2.40	5.89
3	150	100	89.8	2.27	3.28
4	150	100	89.0	2.44	2.04
5	30	22.1	8.02	2.20	n.d.
	45	61.4	33.0	7.20	n.d.
	60	82.5	51.5	13.04	n.d.
	90	98.7	75.1	10.3	n.d.
	120	100	84.0	2.60	n.d.
	150	100	88.7	2.15	1.53

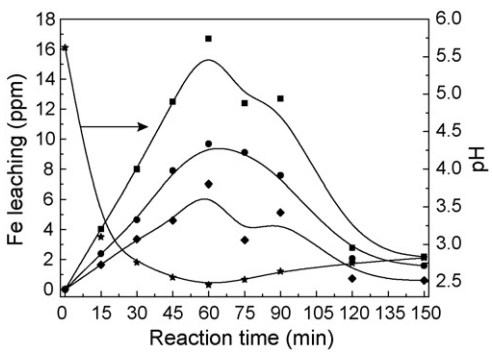

Fig. 11. Evolution of Fe leaching and pH along reaction time in CWO of phenol with the hydrochloric acid treated $ZnFe_{0.25}Al_{1.75}O_4$ catalyst (■, Fe leaching; ●, Fe^{2+} leaching; ♦, Fe^{3+} leaching; ⋆, pH).

confirmed by the evolution of Fe^{3+} and Fe^{2+} leaching from the $ZnFe_{0.25}Al_{1.75}O_4$ catalyst, which was first treated by 1 M hydrochloric acid. In Fig. 11, between reaction time of 75 and 90 min an increase in Fe^{3+} species and a decrease in Fe^{2+} species were observed. The two values were exactly the same indicating that the Fe^{3+} species of increasing came from the Fe^{2+} species of decreasing. But the reason why the Fe^{3+} species cannot be adsorbed between the times is unknown. The similar trend of Fe leaching for this catalyst observed in Fig. 7 implies that the phenomenon is not due to experimental error.

The similar results of the evolution of iron leaching within reaction time were also observed for some other iron-containing catalysts [12,33]. In photocatalytic degradation of formic acid using Fe/TiO_2 catalysts [33], the continues decreases of iron leaching after the maximum concentrations were measured were explained by considering that the presence of remaining Fe_2O_3 acts as crystallization nuclei that facilitates the dissolved iron return as Fe_2O_3. The observed phenomena in this work can be also explained by this conclusion. Another possible hypothesis is that the Fe^{3+} cations can incorporate into the surface octahedral vacancies of the $ZnFe_{2-x}Al_xO_4$ catalysts. Though there is no evidence to confirm these mechanisms, the fact that ferric oxides are important environment adsorbents is well known. They can immobilize metals or ligands via sorption, incorporation, or oxidation–reduction [34]. The rate of iron decreasing is influenced by some intermediate compounds. As shown in Fig. 12, when the process was carried out with the $ZnFe_{0.25}Al_{1.75}O_4$ catalyst in acetic acid solution (pH 2.50), which is one of the main intermediate compounds during phenol degradation, the amount of iron leaching kept unchanged at about 5.7 ppm. During the reaction carried out in blank reaction solution, in which less intermediate compounds were present, the amount of iron leaching decreased nearly to zero. During the two reactions, the initial concentrations of iron leaching are 5.5 and 5.7 ppm, respectively, which are much lower than the maximum iron leaching during phenol oxidation with the S5 catalyst.

Phenol degradation using iron-containing catalysts has been known to proceed via a redox mechanism involving Fe^{3+}/Fe^{2+} redox pair. Hence, the stability of reduced Fe^{2+} species toward acid dissolution is more important, since Fe^{2+} species has a weaker interionic force with O^{2-} than Fe^{3+} species. When Fe^{3+} species is reduced to Fe^{2+} species, it becomes more easily leached out to the solution. As it has been mentioned, the Fe^{3+} cations coordinated in octahedral sites had a strong stability towards acid dissolution, either in hydrochloric acid solution at room temperature or in acetic acid solution at 160 °C. During the two experiments no reaction took place. However, looking at the stability of the catalyst during phenol degradation, as shown in Fig. 7, a significant increase of iron leaching was observed; in Fig. 11, even after the catalyst was treated in 1 M hydrochloric acid solution (the extra framework iron has been removed), the amount of iron leaching was still similar to that with the

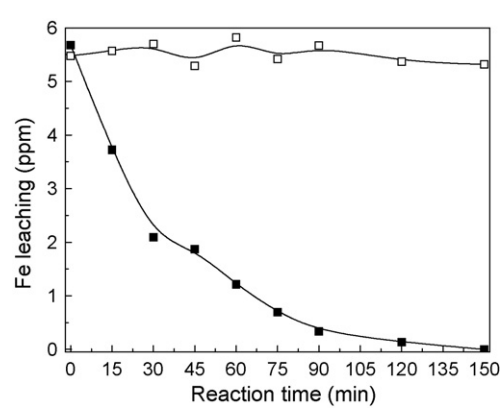

Fig. 12. Evolution of Fe leaching along reaction time with $ZnFe_{0.25}Al_{1.75}O_4$ catalyst in acetic acid solution and in blank reaction solution (■, blank reaction solution and □, acetic acid solution).

untreated catalyst. From these results, it can be deduced that the reduction of Fe^{3+} species can result in an increase of iron leaching. In Fig. 11 it can be also observed that the amount of Fe^{2+} leaching was larger than that of Fe^{3+} leaching. Although this result cannot prove directly the above conclusion, as the leached Fe^{3+} species can take part in the reaction and can be reduced to Fe^{2+} species; nevertheless, it demonstrates that the reduced Fe^{2+} was present and was not easy to be reoxidized to Fe^{3+} before phenol was completely removed. Thus, it is necessary to further search suitable metal ions introduced into the spinel structure to stabilize the reduced oxidation state of iron species. If the rate of reoxidation of reduced iron species on the catalysts surface or of dissolved Fe^{2+} species in solution increased, a significant enhancement in catalyst stability to leaching could be obtained.

4. Conclusions

The activity and stability of $ZnFe_{2-x}Al_xO_4$ spinel catalysts in catalytic wet oxidation of phenolic solution depend on the nature of iron species. Increasing with aluminum content, the main iron species present on the catalyst surface turned from aggregated iron oxide clusters to Fe^{3+} species in octahedral sites. Accordingly, phenol degradation induction period first increased from 30 to 180 min, and then decreased to 5 min. Under acidic conditions, the extraframework iron clusters were easily removed but the Fe^{3+} species incorporated into octahedral sites were stable towards acid dissolution. However, during phenol reaction the reduced Fe^{2+} species in octahedral sites became labile, and resulted in an increase of iron leaching. Within reaction time, the amount of iron leaching first increased to the maximum values at the same time when phenol was completely degraded, and then decreased. In this case the catalysts can be reused for several times with insignificant loss in activity.

Acknowledgements

This work was supported by the National High Technology Research and Development Program of China (no. 2002AA601260). The authors thank Professor Y.G. Liu at the Liaoning Normal University for doing ICP experiments.

References

[1] J.A. Zazo, J.A. Casas, A.F. Mohedano, J.J. Rodríguez, Catalytic wet peroxide oxidation of phenol with a Fe/active carbon catalyst, Appl. Catal. B: Environ. 65 (2006) 261.
[2] S. Perathoner, G. Centi, Wet hydrogen peroxide catalytic oxidation (WHPCO) of organic waste in agro-food and industrial streams, Top. Catal. 33 (2005) 1.
[3] F. Martínez, G. Calleja, J.A. Melero, R. Molina, Heterogeneous photo-Fenton degradation of phenolic aqueous solutions over iron-containing SBA-15 catalyst, Appl. Catal. B: Environ. 60 (2005) 181.
[4] A. Santos, P. Yustos, A. Quintainilla, G. Ruiz, F. Garcia-Ochoa, Study of the copper leaching in the wet oxidation of phenol with CuO-based catalysts: causes and effects, Appl. Catal. B: Environ. 61 (2005) 323.
[5] C. Walling, Fenton's reagent revisited, Acc. Chem. Res. 8 (1975) 125.
[6] A. Cuzzola, M. Bernini, P. Salvadori, A preliminary study on iron species as heterogeneous catalysts for the degradation of linear alkylbenzene sulphonic acids by H_2O_2, Appl. Catal. B: Environ. 36 (2002) 231.
[7] K. Fajerwerg, H. Debellefontaine, Wet oxidation of phenol by hydrogen peroxide using heterogeneous catalysis Fe-ZSM-5: a promising catalyst, Appl. Catal. B: Environ. 10 (1996) L229.
[8] G. Ovejero, J.L. Sotelo, F. Martinez, J.A. Melero, L. Gordo, Wet peroxide oxidation of phenolic solutions over different iron-containing zeolitic materials, Ind. Eng. Chem. Res. 40 (2001) 3921.
[9] J.A. Melero, G. Calleja, F. Martínez, R. Molina, K. Lázár, Crystallization mechanism of Fe-MFI from wetness impregnated Fe_2O_3–SiO_2 amorphous xerogels: role of iron species in Fenton-like processes, Micropor. Mesopor. Mater. 74 (2004) 11.
[10] E. Guelou, J. Barrault, J. Fournier, J.-M. Tatibouet, Active iron species in the catalytic wet peroxide oxidation of phenol over pillared clays containing iron, Appl. Catal. B: Environ. 44 (2003) 1.
[11] J. Guo, M. Al-Dahhan, Catalytic wet air oxidation of phenol in concurrent downflow and upflow packed-bed reactors over pillared clay catalysts, Chem. Eng. Sci. 60 (2005) 735.
[12] A. Bozzi, T. Yuranova, J. Mielczarsky, A. Lopez, J. Kiwi, Abatement of oxalates catalyzed by Fe-silica structured surfaces via cyclic carboxylate intermediates in photo-Fenton reactions, Chem. Commun. (2002) 2202.
[13] R.M. Liou, S.H. Chen, M.Y. Hung, C.S. Hu, J.Y. Lai, Fe(III) supported on resin as effective catalyst for the heterogeneous oxidation of phenol in aqueous solution, Chemosphere 59 (2005) 117.
[14] J. Guo, M. Al-Dahhan, Activity and stability of iron-containing pillared clay catalysts for wet air oxidation of phenol, Appl. Catal. A: Gen. 299 (2006) 175.
[15] Y. Wang, Q. Zhang, T. Shishido, K. Taikehira, Characterizations of iron-containing MCM-41 and its catalytic properties in epoxidation of styrene with hydrogen peroxide, J. Catal. 209 (2002) 186.
[16] N. Crowther, F. Larachi, Iron-containing silicalites for phenol catalytic wet peroxidation, Appl. Catal. B: Environ. 46 (2003) 293.
[17] B. Lavina, G. Salviulo, A.D. Giusta, Cation distribution and structure modelling of spinel solid solutions, Phys. Chem. Miner. 29 (2002) 10.
[18] J.A. Toledo, M.A. Valenzuela, P. Bosch, H. Armendáriz, A. Montoya, N. Nava, A. Vázquez, Effect of AI^{3+} introduction into hydrothermally prepared $ZnFe_2O_4$, Appl. Catal. A: Gen. 198 (2000) 235.
[19] A. Alejandre, F. Medina, X. Rodriguez, P. Salagre, J.E. Sueiras, Preparing and activity of Cu–Al mixed oxides via hydrotalcite-like precursors for the oxidation of phenol aqueous solutions, J. Catal. 188 (1999) 311.
[20] A. Alejandre, F. Medina, A. Fabregat, P. Salagre, J.E. Sueiras, Characterisation of copper catalysts and activity for the oxidation of phenol aqueous solution, Appl. Catal. B: Environ. 18 (1998) 307.
[21] A. Alejandre, F. Medina, X. Rodriguez, P. Salagre, Y. Cesteros, J.E. Sueiras, Cu/Ni/Al layered double hydroxides as precursors of catalysts for the wet air oxidation of phenol aqueous solutions, Appl. Catal. B: Environ. 30 (2001) 195.
[22] A. Xu, M. Yang, H. Du, C. Sun, Influence of partial replacement of Cu by Fe on the CWO of phenol in the $Cu_{0.5-x}Fe_xZn_{0.5}Al_2O_4$ spinel catalysts, Catal. Commun. 7 (2006) 513.
[23] F. Li, J. Liu, D.G. Evans, X. Duan, Stoichiometric synthesis of pure MFe_2O_4 (M = Mg, Co, and Ni) spinel ferrites from tailored layered double hydroxide (hydrotalcite-like) precursors, Chem. Mater. 16 (2004) 1597.
[24] M. Noorjahan, V.D. Kumari, M. Subrahmanyam, L. Panda, Immobilized Fe(III)-HY: an efficient and stable photo-Fenton catalyst, Appl. Catal. B: Environ. 57 (2005) 291.
[25] J.A. Toledo, P. Bosch, M.A. Valenzuela, A. Montoya, N. Nava, A. Vázquez, Oxidative dehydrogenation of 1-butene over Zn–Al ferrites, J. Mol. Catal. A: Chem. 125 (1997) 53.
[26] Y. Sun, S. Walspurger, J.-P. Tessonnier, B. Lousis, J. Sommer, Highly dispersed iron oxide nanoclusters supported on ordered mesoporous SBA-15: a very active catalyst for Fridel–Crafts alkylations, Appl. Catal. A: Gen. 300 (2006) 1.
[27] M.A. Valenzuela, P. Bosch, J. Jiménez-Becerrill, O. Quiroz, A.I. Páez, Preparation, characterization and photocatalytic activity of ZnO, Fe_2O_3 and $ZnFe_2O_4$, J. Photochem. Photobilol. A 148 (2002) 177.
[28] S. Bordiga, R. Buzzoni, F. Geobaldo, C. Lamberti, E. Giamello, A. Zecchina, G. Leofanti, G. Petrini, G. Tozzola, G. Vlaic, Structure and reac-

tivity of framework and extraframework iron in Fe-silicalite as investigated by spectroscopic and physicochemical methods, J. Catal. 158 (1996) 486.

[29] J.-P. Jacobs, A. Maltha, J.G.H. Reintjes, J. Drimal, V. Ponec, H.H. Brongersma, The surface of catalytically active spinels, J. Catal. 147 (1994) 294.

[30] M.A. Valenzuela, J.-P. Jacobs, P. Bosch, S. Reijne, B. Zapata, H.H. Brongersma, The influence of the preparation method on the surface structure of $ZnAl_2O_4$, Appl. Catal. A: Gen. 148 (1997) 315.

[31] A. Bozzi, T. Yuranova, J. Mielczarsky, A. Lopez, J. Kiwi, Evidence for immobilized photo-Fenton degradation of organic compounds on structured silica surfaces involving Fe recycling, New J. Chem. 28 (2004) 519.

[32] F.E. Massoth, D.A. Scarpiello, Catalyst characterization studies on the Zn–Cr–Fe oxide system, J. Catal. 21 (1971) 294.

[33] J. Araña, O. González Díaz, M. Miranda Saracho, J.M. Doña Rodríguez, J.A. Herrera Melián, J. Pérez Peña, Photocatalytic degradation of formic acid using Fe/TiO_2 catalysts: the role of Fe^{3+}/Fe^{2+} ions in the degradation mechanism, Appl. Catal. B: Environ. 32 (2001) 49.

[34] J.H. Jang, B.A. Dempsey, G.L. Catchen, W.D. Burgos, Effects of Zn(II), Cu(II), Mn(II), Fe(II), NO_3^-, or SO_4^{2-} at pH 6.5 and 8.5 on transformations of hydrous ferric oxide (HFO) as evidenced by Mossbauer spectroscopy, Colloids Surf. A: Physicochem. Eng. Aspects 221 (2003) 55.